



## Epithelial-mesenchymal transition induced by MyoD inhibits growth of high metastatic colorectal cancer

Huapeng Sun<sup>a,1</sup>, Aixia Tian<sup>b,1</sup>, Jin Zhang<sup>c</sup>, Xiaofeng Liao<sup>a</sup>, Na Zhang<sup>d,\*</sup>

<sup>a</sup> Department of General Surgery, Xiangyang Central Hospital, Affiliated Hospital of Hubei University of Arts and Science, Xiangyang 441021, Hubei, China

<sup>b</sup> Digestive Department, Xiangyang Central Hospital, Affiliated Hospital of Hubei University of Arts and Science, Xiangyang 441021, Hubei, China

<sup>c</sup> Department Surgery, Hubei Province Nanzhang County Hospital of Traditional Chinese Medicine, Xiangyang 441021, Hubei, China

<sup>d</sup> Pathology Department, Xiangyang Central Hospital, Affiliated Hospital of Hubei University of Arts and Science, Xiangyang 441021, Hubei, China

### ARTICLE INFO

#### Keywords:

Colon cancer  
Myogenicity differentiation factor  
High metastatic  
Epithelial-mesenchymal transition  
E-cadherin

### ABSTRACT

**Objectives:** The study aimed to investigate the tumor-suppressing factor myogenicity differentiation factor (MyoD) against high metastatic colorectal cancer through its powerful transformation by which the tumor cells were converted into muscle cells or other cells to inhibit the malignant proliferation of tumor cells.

**Methods:** The roles of MyoD in colon cancer proliferation, invasion and migration were analyzed by CCK-8 assay and Transwell, and EMT by real-time PCR and Western blot. The secretion of TGFβ1 was assayed by ELISA and activation of p-Smad2/3 were assayed by western blot. The effects of MyoD on intestinal cancer growth and EMT *in vivo* were also analyzed.

**Results:** We found MyoD inhibited the proliferation, invasion and migration of colon cancer cell. Moreover, MyoD inhibited the expression of E-cadherin and promoted the expression of vimentin and α-SMA. The secretion of TGFβ1 increased and p-Smad2/3 was activated after MyoD expression. MyoD also inhibits intestinal cancer growth and promoted EMT *in vivo*.

**Conclusion:** Our findings indicate that MyoD inhibited cancer progression and metastasis by promoting EMT through TGF-β1/Smad2/3 activation, which provide new support for MyoD maybe as a novel anti-cancer method for the treatment of colon cancer in the future.

### Introduction

Malignant tumors cause immeasurable harm to human health which majorly impacts on life. These tumors have a high mortality rate due to their rapid growth, poor differentiation and invasion. Usually, metastasis of malignant tumors is what causes poor prognosis which leads to death in patients with cancers. Tumor cells can acquire phenotypic resemblance to mesenchymal cells through epithelial-mesenchymal transition (EMT), so as to achieve invasive infiltration into surrounding tissues. The normal epithelial cells are neatly arranged in a polar monolayer, and the cells adhere tightly and regularly to each other, and to the extracellular matrix of the basement. Mesenchymal cells have irregular morphology, no polarity and loose intercellular adhesion. They also exhibit migration and infiltration capabilities. EMT not only plays an important role in the invasion and metastasis of tumors, but also correlates with tumor resistance to chemotherapy [14,12].

Theoretically, the number of malignancies spreading to the skeletal

muscle through the blood stream is high due to the abundance of blood vessels in the skeletal muscles. This mostly occurs during strenuous exercise when the blood vessels in muscles are fully engorged with blood. However, some studies have reported that the number of tumors metastasizing to the skeletal muscles is low. Other studies on back this statement since they posit that the cells of skeletal muscles may synthesize and secrete certain tumor suppressing substances which have a wide inhibitory effect on malignant tumor cells [1,10]

Myogenicity differentiation factor (MyoD), one of the four members of the myogenic regulatory factor family (MyoD, MRF5, myo-genin, MRF4), plays an important role in the transcriptional regulation of muscle-specific genes. It also regulates the promoter regions of myo-genin, creatine kinase (CK), myosin, desmin, thus promoting their transcription. Currently, the MyoD-mediated muscle differentiation model is one of the best models for studying cell differentiation [5,4].

Besides promoting the transformation of muscle satellite cells from stationary phase to myoblasts, MyoD also transforms many types of

\* Corresponding author.

E-mail address: [jingyangsdu@126.com](mailto:jingyangsdu@126.com) (N. Zhang).

<sup>1</sup> Huapeng Sun and Aixia Tian made same contribution.

cells such as fibroblasts and adipocytes into myoblasts. It also promotes further integration and differentiation of myoblasts into mature muscle fibers. Studies have confirmed that the high expression of MyoD in chicken, mouse, human fibroblasts and adipocytes can promote the conversion of fibroblasts and adipocytes into myoblasts and the formation of myotubes through gene transfection [9,2].

In summary, we hypothesized that the tumor-suppressing substance, MyoD, inhibits the growth of certain tumor cells or causes their death. This hypothesis was based on its powerful transformation abilities through which certain tumor cells are converted into muscle cells or other cells to inhibit the malignant proliferation of tumor cells. Therefore, this study focused on investigating whether the over expression of MyoD had a transformation effect, inhibitory effect or killing effect on highly metastatic colorectal cancer including its related molecular mechanisms.

## Materials and methods

### HT29 cell culture

The well-grown HT29 cells were prepared and cultured to 80% confluence after digesting them with 0.25% trypsin in a 6-well plate. The normal cells were used as a blank control, while the empty-vector group was used as a negative control. After 4–6 h, the transfection complex was discarded, and a fresh culture medium containing 15% fetal bovine serum (FBS) was added to continue the culture for another 48 h. The cells were subjected to G418 screening to obtain a cell line stably expressing MyoD.

### CCK-8 assay for cell viability

The cells of each group were plated into 96-well plates with 6 replicates in each group. CCK-8 reagent was then added at intervals of 24 h after plating, and the absorbance (A450) was measured at 450 nm in a plate reader [8].

### Transwell cell migration and invasion

The cell concentration was adjusted to  $1 \times 10^5$  cells/ml and 300  $\mu$ l of cell suspension was added to the transwell upper chamber. An additional 700  $\mu$ l of Roswell Park Memorial Institute (RPMI) medium 1640 containing 10% FBS was added to transwell lower chamber at 37 °C in 5% CO<sub>2</sub> and cultured for 48 h. The Transwell chamber was taken out and the liquid discarded. A cotton swab was used to wipe the internal basement membrane. Subsequently, the PBS was rinsed and fixed with 4% paraformaldehyde for 10 min. Staining was done with crystal violet for 20 min and then rinsed with clear water. The result was then observed under the microscope. Invasion experiments were performed by mixing liquid BD matrigel with serum-free medium (1:5) and adding 400  $\mu$ l into the upper chamber of Transwell. It was then placed in a cell culture incubator for 2 h in which led to the production of a thin layer gel. Other subsequent steps were similar to the migration experiment.

### Real-time PCR

Total RNA was extracted from the cells using Trizol. After measuring the concentration, 1  $\mu$ g of total RNA was used for reverse transcription. Real-time fluorescence quantitative PCR was performed using GAPDH as an internal reference using the 20  $\mu$ l system according to the Fast SYBR™ Green Master Mix (Thermo Fisher Scientific, USA). PCR reaction scheme was as follows: 95 °C, 5 min; 40 cycles of 95 °C, 10 s, 60 °C, 30 s and 72 °C, 20 s. Lastly, 95 °C, 5 s and 65 °C, 1 min. The primers were designed and synthesized by Beijing Saibaisheng Company. The relative expression of mRNA was calculated using the formula  $2^{-\Delta\Delta CT}$  [13].

### Western blotting

Total protein was extracted using RIPA and 30  $\mu$ g was applied to SDS-PAGE. It was then transferred to PVDF membrane. After the membrane was blocked by TBST (containing 5% skim milk) for 2 h and washed by TBST for 4 times  $\times$  5 min, polyclonal rabbit anti-vimentin (1:200), E-cadherin (1:250),  $\alpha$ -actin antibody, MyoD antibody, and GAPDH (1:1000) were added to incubate overnight at 4 °C. After washing the membrane, the corresponding secondary antibody was added to incubate for 2 h at room temperature followed by TBST washing for 3 times. The results were detected by ECL luminescence in dark room. All antibodies were purchased from Santa Cruz Biotech, Dallas, Texas, USA. Grayscale analysis of bands was performed using Image J software. Semi-quantitative analysis was performed using GAPDH as an internal control, and the value was determined by the ratio of the target band to the gray value of the corresponding GAPDH [11].

### Establishment of nude mouse xenograft model and observation of tumor growth

The study was approved by Xiangyang Central Hospital (XYCH-2016-51) and carried out in strict accordance with the recommendations in the Guide for the Care and Use of Laboratory Animals of Institutes of Health. All efforts were made to minimize risks.

Twelve BALB/C nude mice, 4–6 weeks old, female, weighing 18–22 g were provided by the laboratory animal center and fed standardly at a constant temperature of 18–22 °C, constant humidity of 50% to 80%, and a closed sterile environment with free intake of sterile water. Twelve BALB/C nude mice were divided into three groups: those inoculated with wild-type HT29 cells, empty-vector transfected cells, and MyoD-expressing HT29 cells. The MyoD vector carried a green fluorescent protein gene as a marker. At 1 day before tumorigenesis, the cells in the logarithmic growth phase with 90% confluency were digested and diluted to  $1 \times 10^6$  in 200  $\mu$ l saline. They were then injected into the bilateral groin of nude mice – 0.2 ml was injected on each side. The growth of the tumor and the survival of the nude mice were continuously observed from 15th day since they are normally reared for 30 days. The long diameter and short diameter of the tumor were measured with a vernier caliper. The tumor volume and tumor inhibition rate were calculated using the formula: Tumor volume =  $1/2$  long diameter  $\times$  short diameter  $^2$ ; Tumor inhibition rate =  $(1 - \text{experimental group mean tumor volume/control mean tumor volume}) \times 100\%$ .

After 30 days of inoculation, the nude mice were injected isoflurane overdose and given cervical dislocation. The subcutaneous tumor tissues were completely isolated and fixed in formaldehyde. PCNA immunohistochemistry was performed. The PCNA level reflected the proliferation of cancer cells. The integral optical density (IOD) values of PCNA were measured by CMIAS-8 color pathological image analysis system.

### Statistical analysis

Statistical analysis was performed with SPSS 18.0 software. Hence, data was expressed as mean  $\pm$  standard deviation, compared by paired sample *t*-test or independent sample *t*-test, and the difference was significant with a *p* value, *p* < 0.05.

## Results

### MyoD inhibited cell proliferation and migration

As shown in Fig. 1A, the fluorescence in empty vector or MyoD-transfected HT29 cells was significantly increased under the fluorescence microscope. The qRT-PCR assay also showed that the MyoD

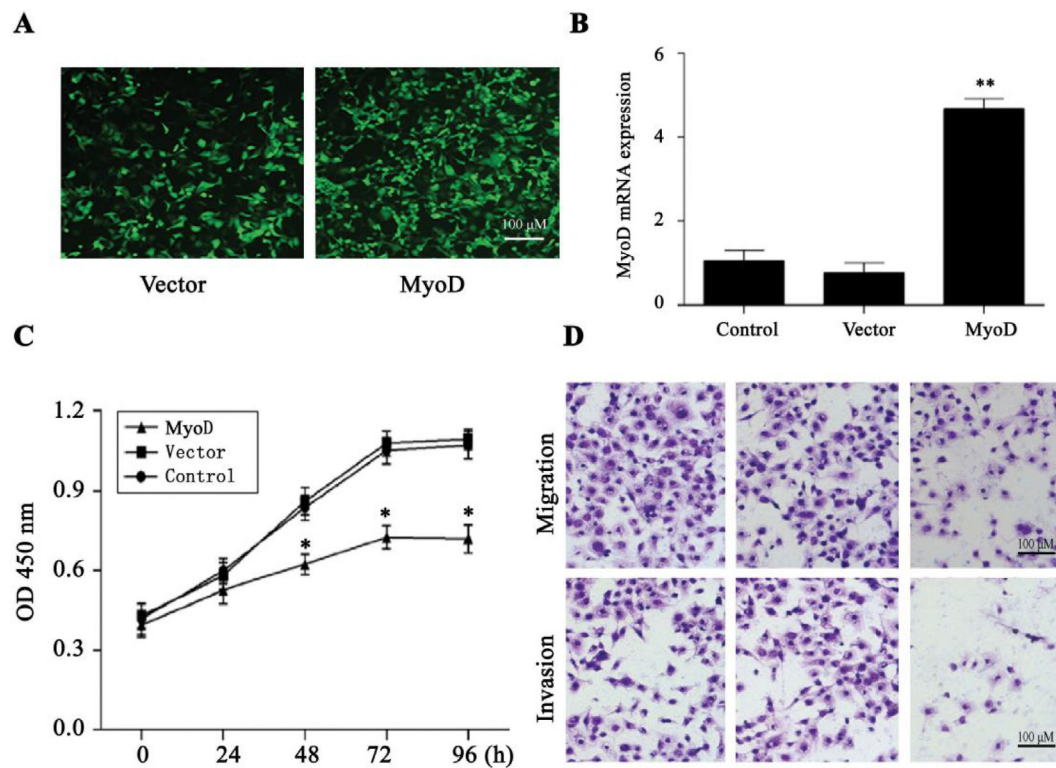


**Fig. 1.** Effect of MyoD on cell proliferation and migration (n = 6). A, the transfected cells were assayed by fluorescence microscope; B, MyoD expression was assayed by Real-time PCR; C, cell proliferation was assayed by CCK-8; D, invasion and migration were assayed by transwell chamber.

expression level in the MyoD-expressing cells was significantly higher than that in the empty-vector group (Fig. 1B,  $p < 0.01$ ).

As shown in Fig. 1C, CCK-8 results showed that compared with the control group, the cell proliferation ability of the group expressing MyoD was significantly lower than that of the control group at 24, 48, 72, 96 h ( $p < 0.01$ ). This was a clear indication that the growth rate of cells in MyoD-expressing group was inhibited.

As shown in Fig. 1D, the results of Transwell experiments showed the migration and invasion ability of MyoD-expressing group decreased when compared to the control group. This showed that the expression of MyoD significantly inhibited the migration and invasion of HT29 cells.

#### MyoD promoted EMT of HT29 cells

qRT-PCR results showed that the E-cadherin mRNA level was down-regulated in the MyoD-expressing group contrary to what was evident in the control group. The expression of both vimentin mRNA and the myofibroblast marker  $\alpha$ -SMA mRNA were significantly upregulated ( $p < 0.05$ ) (Fig. 2A); Western blotting showed that E-cadherin expression in the MyoD-expressing group decreased ( $p < 0.05$ ), while vimentin and  $\alpha$ -SMA protein expression increased ( $p < 0.05$ ). This led to the suggestion that MyoD can induce HT29 cell differentiation to myofibroblasts (Fig. 2B).

#### MyoD promoted EMT through TGF- $\beta$ 1/Smad2/3 activation

The TGF $\beta$ 1/Smad2/3 pathway significantly facilitates EMT in various epithelial cells. We speculated that it could be a potential mechanism for MyoD to induce EMT in cells. Consequently, we used ELISA to detect the secretion of TGF $\beta$ 1 in cell culture supernatant. The ELISA results indicated that the concentration of TGF $\beta$ 1 in the supernatant of MyoD group was approximately 2-fold higher than that of the control group ( $p < 0.01$ ) (Fig. 3A). The Smad2/3 phosphorylation was detected

by Western blot. The results also showed that the p-Smad2/3 in the MyoD group was significantly higher than that of the control group ( $p < 0.05$ ) (Fig. 3B).

#### MyoD inhibits intestinal cancer growth in vivo

After 30 days of continuous observation, we found that the growth rate of the group expressing MyoD was significantly lower than that of the empty vector group. Tumors in MyoD group grew slower than tumors in empty vectors ( $p = 0.00021$ , Fig. 4A). After the mice were sacrificed, the tumor tissues were detected by immunocytochemical staining and real-time PCR. Real-time PCR showed that MyoD was highly expressed in the MyoD-expressing group (Fig. 4B). PCNA staining confirmed that the tumors in the MyoD group were weaker than those from the empty vector group (Fig. 4C). The real-time PCR also showed E-cadherin mRNA level was down-regulated and both vimentin and  $\alpha$ -SMA mRNA were significantly upregulated (Fig. 4D), thereby suggesting that MyoD inhibited the growth of tumors through cell differentiation into myofibroblasts *in vivo*.

#### Discussion

Tumor cells undergo EMT in three processes associated with changes in cell morphology. That is, the epithelial cells lose polarity and intercellular adhesion making them appear like irregular and loosely arranged interstitial cells. Moreover, certain changes are noticed in cell surface markers. For instance, the epithelial cell marker, E-cadherin, decreased while interstitial cell marker vimentin and fibrin were up-regulated. Additionally, changes in cell biological behavior are also evident. In this regard, epithelial cells changed from a static state to metastatic interstitial cells with strong infiltration capacity, making them acquire interstitial phenotype of invasiveness and anti-apoptotic capacity [3].

MyoD is a transcription factor with a three-dimensional crystal

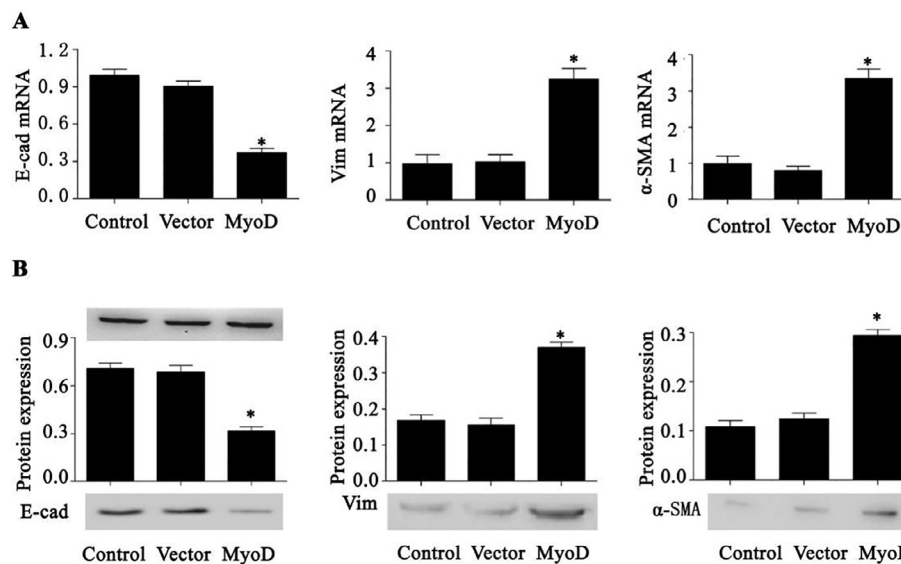


Fig. 2. The expression levels of E-cadherin, vimentin and α-SMA were assayed by qRT-PCR (n = 6, A) and Western blotting (n = 5, B).

structure of a basic helix-loop-helical domain. This domain binds to other proteins with a helix-loop-helical domain such as myocyte-promoting factor 2 (MEF2), myogenin, and creatine kinase (CK), whose adjacent basic region is a domain necessary for binding to the promoter or enhancer of many muscle-specific gene DNA (CK, myogenin, etc.). Its amino terminus also has two domains-histidine cysteine (H/C) and transcriptional activation domain (AD). These two domains are involved in the transcriptional activation of the MyoD target genes. Its carboxyl end is the facultative D helix III domain which may be related to chromatin remodeling [6]. The research results showed that MyoD has the ability to promote the morphological changes of tumor cells, and EMT differentiation to myofibroblasts thus changing the biological characteristics of tumor cells.

The TGF-β1/Smad pathway is a classical signaling pathway for EMT. Epithelial cells play an important role in EMT and fibrosis through the TGF-β1/Smad pathway. Activation of the TGF-β1/Smad pathway enhances cell adhesion and migration. It also promotes microvascular angiogenesis by increasing VEGF expression [7]. This study showed that high expression of MyoD promoted the activation of TGF-β1 and Smad signaling pathways, but inhibited the proliferation, migration and invasion.

In conclusion, this finding suggests that MyoD may inhibit tumor growth by altering cell biological properties.

**Declarations**

*Ethics approval and consent to participate*

The study was approved by Xiangyang Central Hospital (XYCH-2016-51).

*Consent for publication*

N/A.

*Availability of data and material*

All datasets on which the conclusions of the manuscript rely were presented in the text.

*Funding*

N/A.

*Authors' contributions*

SH, TA, ZJ and LX carried out the studies. ZN participated in the design of the study and performed the statistical analysis. All authors read and approved the final manuscript.

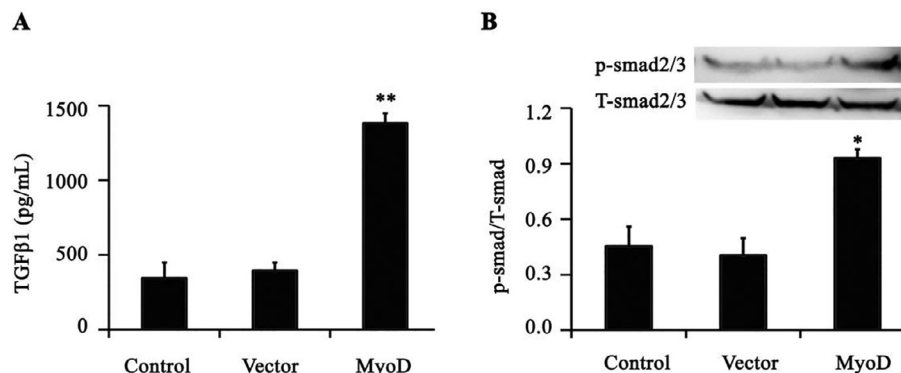


Fig. 3. MyoD regulates EMT-related molecules in HT29 cells through TGF-β1/Smad2/3 activation (n = 6). A, the secretion of TGFβ1 in cell culture supernatant was assayed by ELISA; B, p-Smad2/3 and total-Smad2/3 were assayed by Western blot.

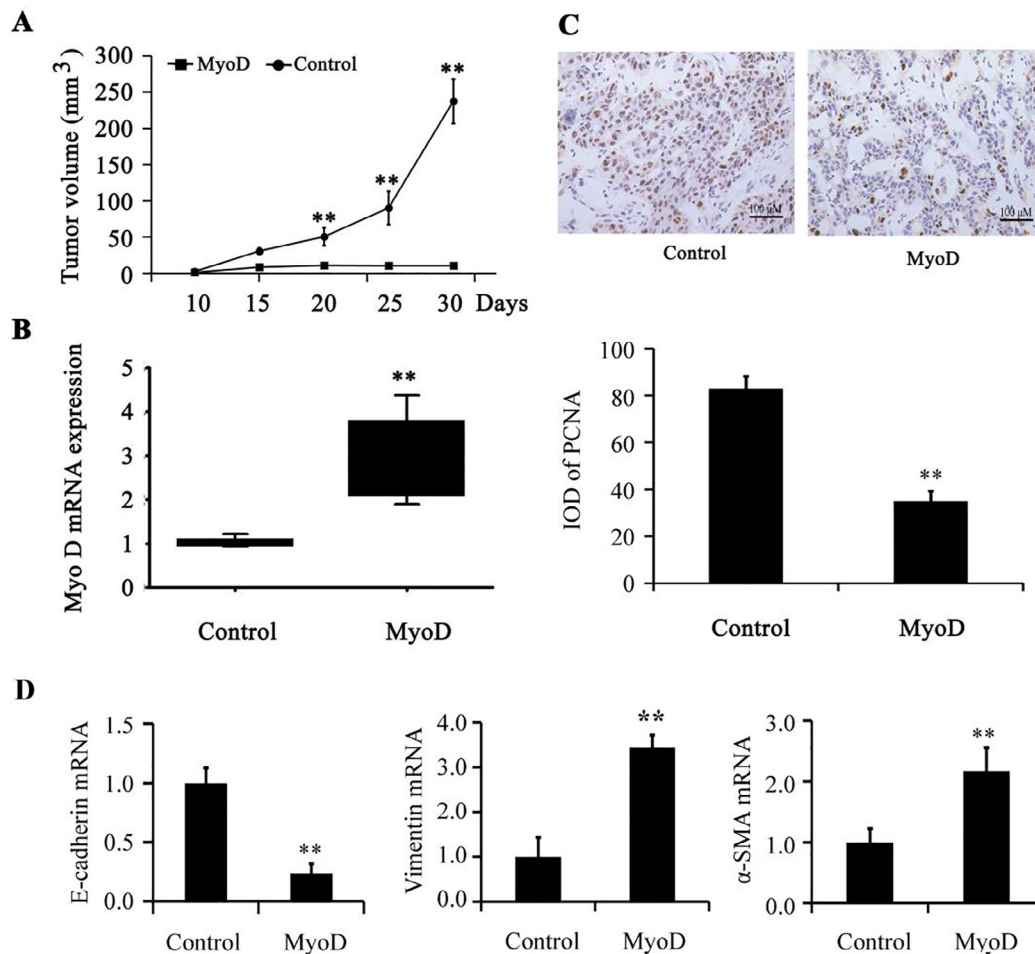


Fig. 4. MyoD suppresses lung cancer growth *in vivo*. A, tumor growth; B, Myo D expression by real-time PCR; C, PCNA staining. D, E-cadherin, vimentin and α-SMA were assayed by qRT-PCR.

**Declaration of Competing Interests**

N/A.

**Acknowledgement**

N/A.

**Appendix A. Supplementary data**

Supplementary data to this article can be found online at <https://doi.org/10.1016/j.mehy.2019.109285>.

**References**

- [1] Bashir U, Qureshi A, Khan HA, Uddin N. Gastrointestinal stromal tumor with skeletal muscle, adrenal and cardiac metastases: an unusual occurrence. *Indian J Pathol Microbiol* 2011;54:362.
- [2] Bichsel C, Neeld D, Hamazaki T, Chang LJ, Yang LJ, Terada N, et al. Direct reprogramming of fibroblasts to myocytes via bacterial injection of MyoD protein. *Cell Reprogram* 2013;15:117.
- [3] Bill R, Christofori G. The relevance of EMT in breast cancer metastasis: correlation or causality? *FEBS Lett* 2016;589:1577–87.
- [4] Blum R, Vethantham V, Bowman C, Rudnicki M, Dynlacht BD. Genome-wide identification of enhancers in skeletal muscle: the role of MyoD1. *Genes Dev* 2012;26:2763–79.
- [5] Cao Y, Yao Z, Sarkar D, Lawrence M, Sanchez GJ, Parker MH, et al. Genome-wide MyoD binding in skeletal muscle cells: a potential for broad cellular reprogramming. *Dev Cell* 2010;18:662–74.
- [6] Forcales SV, Albini S, Giordani L, Malecova B, Cignolo L, Chernov A, et al. Signal-dependent incorporation of MyoD-BAF60c into Brg1-based SWI/SNF chromatin-remodelling complex. *EMBO J* 2012;31:301–16.
- [7] Islam SS, Mokhtari RB, El Hout Y, Azadi MA, Alauddin M, Yeger H, et al. TGF-β1 induces EMT reprogramming of porcine bladder urothelial cells into collagen producing fibroblasts-like cells in a Smad2/Smad3-dependent manner. *J Cell Commun Signal* 2014;8:39–58.
- [8] Li L, Liu M, Kang L, Li Y, Dai Z, Wang B, et al. HHEX: a crosstalk between HCMV infection and proliferation of VSMCs. *Front Cell Infect Microbiol* 2016;30:169.
- [9] Noh OJ, Park YH, Chung YW, Kim IY. Transcriptional regulation of selenoprotein W by MyoD during early skeletal muscle differentiation. *J Biol Chem* 2010;285:40496–507.
- [10] Rao SP, Miller ST, Wrzolek M, Haller JO, Klotz D. Skeletal muscle metastasis in a patient with Wilms tumor and multiple late recurrences. *Cancer* 2015;71:1343–7.
- [11] Qin L, Qiu K, Hu C, Wang L, Wu G, Tan Y. Respiratory syncytial virus promoted the differentiation of Th17 cells in airway microenvironment through activation of Notch-1/Delta3. *J Med Microbiol* 2019;68:649–56.
- [12] Sciacovelli M, Gonçalves E, Johnson TI, Zecchini VR, da Costa AS, Gaude E, et al. Fumarate is an epigenetic modifier that elicits epithelial-to-mesenchymal transition. *Nature* 2016;537:544–7.
- [13] Wang L, Wu G, Qin X, Ma Q, Zhou Y, Liu S, Tan Y. Expression of nodal on bronchial epithelial cells influenced by lung microbes through DNA methylation modulates the differentiation of T-helper cells. *Cell Physiol Biochem* 2015;37:2012–22.
- [14] Zheng X, Carstens JL, Kim J, Scheible M, Kaye J, Sugimoto H, et al. Epithelial-to-mesenchymal transition is dispensable for metastasis but induces chemoresistance in pancreatic cancer. *Nature* 2015;527:525–30.